

UK Magnetism Society

Grove Business Centre Grove Technology Park Wantage Oxfordshire OX12 9FA UK
tel: +44 (0) 1235 770652 fax: +44 (0) 1235 772295 email: mswadling@ukmagsoc.co.uk
www.ukmagsoc.org

CAD for Electromagnetic Devices

One-Day Seminar 2 November 2006 Rolls Royce plc

Finite element modelling of magnetostatics for magnetron sputter sources

Sarah Powell, Gencoa Ltd, Physics Road, Liverpool, L24 9HP, United Kingdom

sarah.powell@gencoa.com, tel: +44 (0) 151 486 4466

Introduction

Vacuum coating processes use a vacuum environment and an atomic or molecular condensable vapour source to deposit thin films, typically $<5\mu\text{m}$ in thickness. An example of such a process is magnetron sputtering where material is removed from a solid target by ion bombardment and deposited on a substrate in atomic layers. It is one of the most flexible and controllable methods of generating a metal vapour in a vacuum. Applications include low friction coatings for tools, anti-reflective coatings on glass, decorative coatings e.g. bath taps, touch panel screens, car headlamps, telescope mirrors and coatings for photovoltaics.

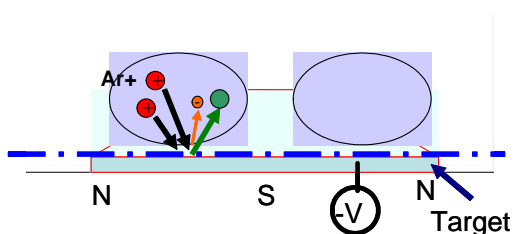


Fig.1 Schematic of magnetron sputtering process.

A magnetron comprises a cathode, an anode and a combined electric and magnetic field as seen in figure 1. There are various types of magnetron depending upon the application and the target efficiency required. Each type requires an optimised design of magnetic field to ensure sound operation of the magnetron source. This is achieved by finite element modelling using the magnetostatic element of Quickfield™ software. Quickfield™ is a very efficient user-friendly finite element analysis package for electromagnetic, thermal, and stress design simulation with coupled multi-field analysis. Analysis of the results is possible in many different graphical forms. The

data from the results files can be exported and used in software developed at Gencoa to simulate target erosion and coating uniformity on substrates. Results have shown good agreement with experimental and theoretical data.

Creating a model

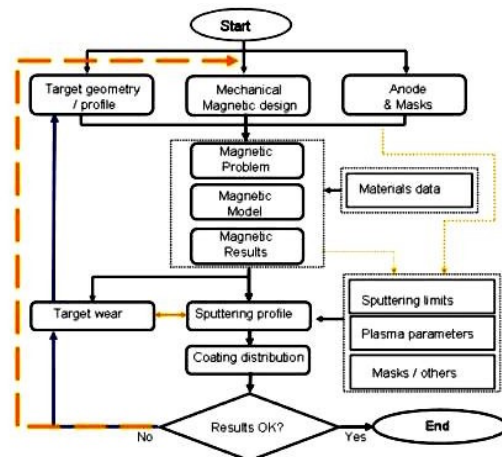


Fig. 2 Modelling process flow chart

When creating a model, several factors must be taken into consideration as can be seen in figure 2 above. These include magnetron size and type, target material, target thickness, process requirements and any ferromagnetic components that may be present in the vacuum chamber. Data can be imported and exported from CAD drawings produced by the design team at Gencoa and this enables the geometry of a model to be created in a model editor in Quickfield™. A materials library is available to assign material properties to each part of the model. The programme automatically generates a mesh suitable to the model geometry and the solver creates a finite element model within minutes, see figures 3 and 4 for examples of a model and mesh. The model opens up in a postprocessor where the results can be analysed.

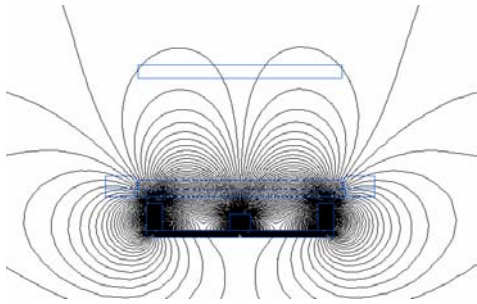


Fig. 3 Example of typical 2-pole magnetic field model for a rectangular magnetron sputter source generated in Quickfield™.

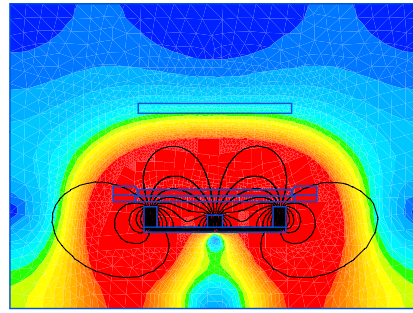


Fig. 6 Colour map of field strength for typical 2 pole rectangular magnetron.

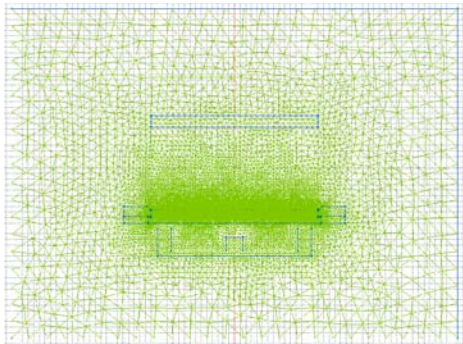


Fig. 4 Example of mesh produced in Quickfield pre-processor.

Model Analysis

Analysis usually consists of mapping the field strength as shown in figures 5 and 6, assessing the field shape over the target and interactions with the anode and substrate and the level of substrate bombardment. Several magnetrons can be modelled together to check complete system interactions (see figures 11 and 12 for plasma view). Data from these models is exported to obtain target erosion profiles and perform coating uniformity simulations. The geometry is often manipulated several times to achieve the best combination of magnetic field shape and strength for the required application.

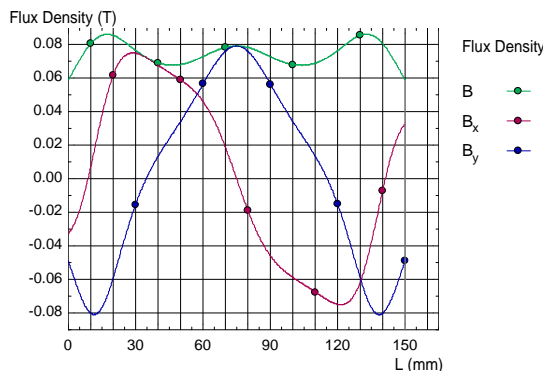


Fig. 5 Field strength over target surface for typical 2 pole rectangular magnetron.

Plasma potential measurements

The models can also be used as a reference when making measurements of plasma potential. In this particular experiment¹ the magnetic field of a 150mm diameter circular magnetron was modelled to give the initial field strengths. A Hall probe was used to confirm these measurements. An emissive probe was placed in the plasma area as seen in figure 7 below. The results in figure 8 show a distinct correlation with the magnetic field distribution obtained in Quickfield™ indicating that the plasma potential is clearly affected by the magnetic field present over the target on the magnetron source

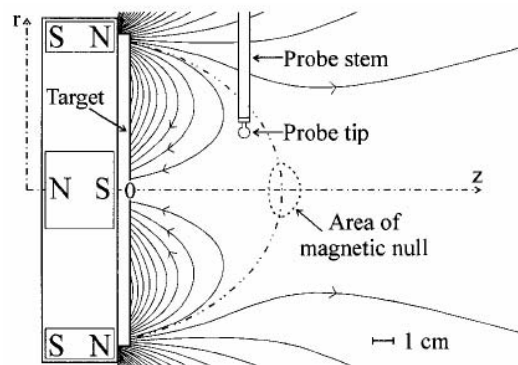


Fig. 7 Schematic diagram of a magnetron plasma source showing magnetic field configuration and emissive probe.

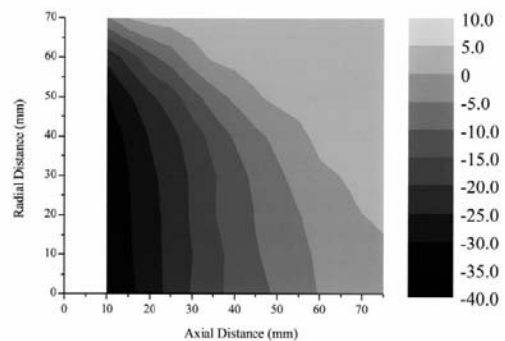


Fig. 8 Graph showing distribution of plasma potential for a discharge pressure of 0.26 Pa and a target bias of -330V.

Balance v. Unbalance

Balanced and unbalanced are terms commonly used in magnetron sputtering. Balanced is generally used to describe conventional magnetrons. Windows and Savvides² were the first people to recognise and classify unbalanced magnetrons.

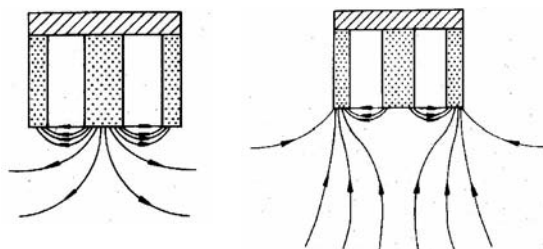


Fig. 9 Type I and Type II magnetrons as described by Windows and Savvides.

The ability of the electrons to escape from the magnetic trap is determined by the position of the null point in the plasma above the target. If the null point is high above the target, there is little chance of electrons escaping and the magnetron is balanced. In this case, there is low ion bombardment on the substrate, assuming the substrate is positioned above the null point. If the null point is close to the target surface, the electrons can escape more easily and the magnetron is unbalanced. Unbalanced designs can produce high ion bombardment of the thin film at the same time as deposition. In figure 9, Type 1 is a balanced design and is characterised by the open field lines extending over and beyond the target surface. Type 2 is an unbalanced design and is characterised by the closed field lines that are confined above the target surface.

Gencoa use a simple method to determine the degree of unbalance and classify magnetrons into 6 groups according to the value of g , which is the ratio, $Z_{Bz=0}/W_{1/2}$ where Z is the distance to the null point and W is the target width. The classification can be seen in table 1 below.

Group Number	Group description	$G=Z_{Bz=0}/W_{1/2}$
I	Extremely balanced	$g \geq 2.00$
II	Very balanced	$1.75 \leq g < 2.00$
III	Middle balanced	$1.5 \leq g < 1.75$
IV	Unbalanced	$1.25 \leq g < 1.5$
V	Very unbalanced	$1.0 \leq g < 1.25$
VI	Extremely unbalanced	$G < 1.0$

Table 1. Magnetron classification

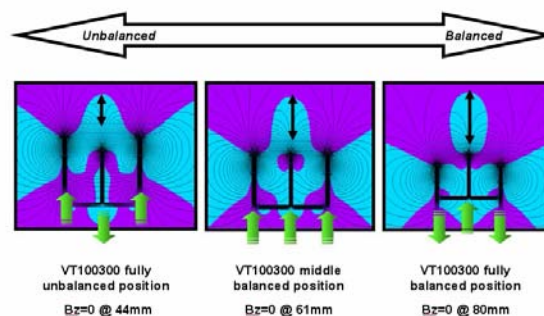


Fig. 10 Levels of balance/unbalance for a V-tech magnetron.

However, ion bombardment can be extremely beneficial for some applications for a number of reasons. It densifies coatings, aids plasma reactivity and compound formation and can also improve coating adhesion. The optimum level of ion bombardment can be found by using a Gencoa V-tech magnetron as shown in figure 10 above. The different models are created by moving the magnets in the Quickfield™ model editor. This determines the correct amount of variation of the magnetic field necessary between highly balanced and highly unbalanced. Once the required level has been achieved, fixed magnetrons can be manufactured for production purposes with the optimum degree of balance or unbalance to create the ideal film structure.



Fig. 11 Plasma shot showing unbalanced effect and linking of plasma for two magnetrons.

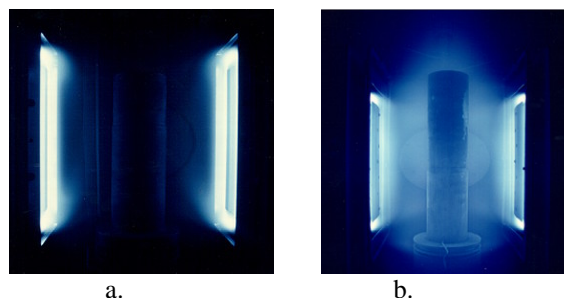


Fig. 12 Effect of magnet polarity on plasma a) same polarity b) opposite polarity

Target Erosion

A programme has been developed that can predict the erosion of the target. This uses data supplied by the finite element modelling of the magnetic field. The software allows direct simulation of the target erosion, eliminating the requirement for a plasma test in the design process. It is particularly effective for two pole designs. Figure 13 below shows the good correlation between theoretical and experimental results for a 6 inch circular magnetron. The point on the target surface where the horizontal component of the magnetic field is zero ($B_z=0$, see colour change below) is the point where the erosion is usually highest.

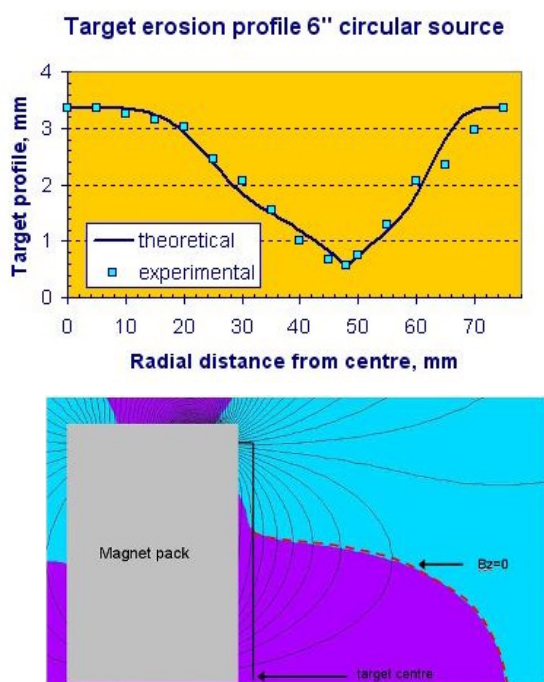


Fig. 13 Experimental and theoretical results for target erosion of a 6 inch circular magnetron.

Coating Uniformity

A program has also been developed that can predict the coating uniformity on a substrate. The program calculates the sputtering probability across the substrate and hence a model of the coating flux from the target material can be generated. Correction factors can be added to the model to account for different target materials, since the angular sputtering dependence varies for each material. The program uses data from the finite element magnetic field modelling and can consider many factors including whether substrates are on or off axis, rotating or not and the required height of the substrate from the source. Also, for a given uniformity requirement, the optimum position of the substrate can be advised.

If the uniformity cannot be achieved then some manipulation of the magnetic field may be required. By using the simulation software it is possible to predict the corresponding change in uniformity as seen in figure 14 below. In this way the uniformity can be tuned to a specific application requirement.

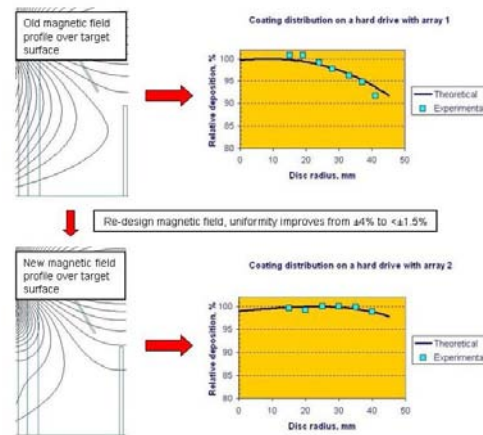


Fig. 14 Comparison of uniformity data before and after manipulation of the magnetic field

Conclusion

In summary, it has been shown that, by using Quickfield™ finite element modelling software, it is possible to create a good representation of the magnetic field shape in a magnetron sputter source, to optimise this magnetic field and also optimise magnetic field strength and the level of balance/unbalance in a magnetron. Using the data from these models, it is also possible to predict target erosion which is an important economic consideration for the customer and coating uniformity that could be critical to the process application.

References

1. J.W. Bradley, S Thompson and Y Aranda Gonsalvo, Plasma Sources Sci. and Technol. 10 (2001) 490-501
2. B. Window and N. Savvides, J. Vac. Sci. Technol. A 4(2), (1986) 196.

Acknowledgements

The author wishes to acknowledge Bill Sproul for supplying the plasma photographs in Figure 10.